



# Quantifying capture and ingestion of live feeds across three coral species

Julia Saper<sup>1,2,3</sup> · Lone Høj<sup>2</sup> · Craig Humphrey<sup>2</sup> · David G. Bourne<sup>1,2</sup>

Received: 12 March 2023 / Accepted: 29 May 2023  
© Crown 2023

**Abstract** Nutrient acquisition through heterotrophy is critical for the health of reef-building corals. The optimization of exogenous nutrition protocols to support a diversity of aquaculture corals requires improved techniques to assess feeding rates. Here, we compared the feeding rates of three coral species (*Acropora millepora*, *Pocillopora acuta* and *Galaxea fascicularis*) fed *Artemia salina* through capture rate (indirect) and dissection (direct) approaches, with direct detection and enumeration within dissected polyps facilitated by fluorescent microbeads ingested by the *Artemia*. When *A. millepora* was provided *Artemia* at 3 individuals ml<sup>-1</sup> for one hour, the calculated capture rates (0.7 ind. polyp<sup>-1</sup> h<sup>-1</sup>) overestimated prey ingested compared to prey detected directly within polyps (0.2 ind. polyp<sup>-1</sup> h<sup>-1</sup>), and ingestion varied significantly between genotypes. In contrast, for *P. acuta*, capture rate calculations (1 ind. polyp<sup>-1</sup> h<sup>-1</sup>) underestimated prey detected within polyps (3.5 ind. polyp<sup>-1</sup> h<sup>-1</sup>) and ingestion did not vary between genotypes. For *G. fascicularis*, the feeding rates were similar as calculated by both capture rates (59 ind. polyp<sup>-1</sup> h<sup>-1</sup>) and by polyp dissections (75 ind. polyp<sup>-1</sup> h<sup>-1</sup>). Results from this study provide valuable insights into coral feeding rates of

different coral species that can improve prey enrichment and feeding strategies for nutritional supplementation of corals in captivity.

**Keywords** Coral feeding · Coral aquaculture · Fluorescence microscopy · *Artemia* · Feeding rates · Dissections

## Introduction

Coral aquaculture is expanding rapidly to supply a growing ornamental trade and to replenish reefs that have been degraded due to anthropogenic impacts (Osinga et al. 2011; Leal et al. 2016). Across the ornamental and hobbyist industry, there are over 100 coral species collected from the wild and propagated in relatively small-scale aquarium systems (Borneman 2009; Tagliafico et al. 2018a). However, as the demand for coral increases, the scale at which corals are cultured in captivity must also expand to reduce impacts of wild harvesting (Barton et al. 2015). Exogenous feeds are needed to fully meet the nutritional needs of captive corals. Our limited understanding of the nutritional requirements of corals and their species-specific feeding abilities represent significant hurdles for large-scale production.

Heterotrophic feeding is essential to the health of all symbiotic, reef-building corals (Brafield & Llewellyn 1982; Anthony & Fabricius 2000; Houlbrèque et al. 2004a). Symbiotic corals are mixotrophs, obtaining energy through autotrophic assimilation of photosynthates derived from their algal symbiotic partners (*Symbiodiniaceae*) and through heterotrophic feeding (Houlbrèque & Ferrier-Pagès, 2009; Ferrier-Pagès et al. 2011). Although some corals can acquire significant amounts of their energy needs from photosynthates, all corals require heterotrophic inputs to survive

**Supplementary Information** The online version contains supplementary material available at <https://doi.org/10.1007/s00338-023-02397-1>.

✉ David G. Bourne  
david.bourne@jcu.edu.au

- <sup>1</sup> College of Science and Engineering, James Cook University, Townsville, QLD 4811, Australia
- <sup>2</sup> Australian Institute of Marine Science, PMB 3 Townsville MC, Townsville, QLD 4810, Australia
- <sup>3</sup> AIMS@JCU, James Cook University, Townsville, QLD 4811, Australia

(Palardy et al. 2008; Hughes et al. 2010; Ezzat et al. 2016). Morphological characteristics can provide useful insights into a coral species' feeding ability. For example, a fast-growing branching or tabulate coral colony, such as an *Acropora* sp., has small polyps (< 1 mm diameter) and the high surface to volume ratios of colonies maximizes light-acquisition which can impede capture of live prey. In contrast, a slow-growing massive coral colony, such as a *Favites* sp., has larger polyps (> 5 mm diameter), which may have evolved to maximize plankton-capture (Houlbrèque et al. 2009; Conti-Jerpe et al. 2020).

Among a range of diets employed by aquarium facilities, *Artemia* spp. nauplii is a cost-effective, commercially available option. *Artemia* is offered to an estimated 85% of all marine organisms in aquaculture (Trager et al. 1994; Sebens et al. 1998; Kumar & Babu 2015) and has been demonstrated to stimulate growth and improve survivability of a range of captive corals (Osinga et al. 2012a; Tagliafico et al. 2018a). The growth and survival of juvenile and adult aquarium reared *Pocillopora acuta* (Toh et al. 2013; Huang et al. 2020), *Pocillopora damicornis* (Conlan et al. 2018), *Acropora tenuis*, *Favia fragum* (Petersen et al. 2008) and *Duncanopsammia axifuga* (Tagliafico et al. 2018b) improved significantly when fed *Artemia* nauplii when compared to unfed corals.

A range of indirect and direct approaches have assessed coral feeding abilities, each with strengths and limitations. The capture rate approach is an indirect method of assessment commonly used to select optimal feeding densities for aquarium reared corals (Osinga et al. 2008, 2012b; Kuanui et al. 2016). Determination of mean capture rates involves counting prey in a fixed volume of water before and after a feeding period and then, normalizing to a unit of coral (e.g., surface area or polyp number). The capture of *Artemia* by a range of corals, including small polyp *Acropora* species (Hoogenboom et al. 2015; Kuanui et al. 2016; Tagliafico et al. 2018a), *P. damicornis* (Hoogenboom et al. 2015; Kuanui et al. 2016) and relatively large polyp *Galaxea fascicularis* (Hii et al. 2009; Osinga et al. 2012b; Hoogenboom et al. 2015) and *D. axifuga* (Tagliafico et al. 2018a), has been measured through this approach. However, such indirect methods rely on problematic assumptions that prey captured equals prey consumed and do not account for the dynamics of prey capture, ingestion and release, or prey passively caught by mucus secretions but not ingested (Osinga et al. 2012b). Additionally, the capture rate approach calculates average capture rates per polyp based on whole fragment measurements, although there is likely a non-uniform distribution of ingested prey across polyps within a fragment and across the larger colony.

To quantify and assess both capture and ingestion of delivered feeds by individual coral polyps, direct approaches must be utilized. Direct approaches can more

accurately assess coral feeding and to date have employed video (Wijgerde et al. 2011; Osinga et al. 2012b) and coral polyp dissections (Hall et al. 2015; Kuanui et al. 2016; Smith et al. 2016). For example, dissections of *P. damicornis*, *A. millepora* and *A. nobilis* polyps have been utilized to investigate the breakdown of *Artemia* nauplii in fed corals as well as the composition of ingested plankton in *G. fascicularis* across reef habitats (Kuanui et al. 2016; Smith et al. 2016; Axworthy & Padilla-Gamino 2019). However, dissections require time, refined microscopic approaches and are complicated by small coral polyps and cryptic prey (Trager et al. 1994; Houlbrèque et al. 2004b). Importantly, though polyp dissections are an important tool to understand the amount and types of prey consumed, it is not always feasible to differentiate degraded prey from coral tissue. One approach to overcome these limitations is visual aids (e.g., dyes, fluorescent markers) to improve prey detection. The addition of fluorescent markers could extend our understanding of feeding by facilitating documentation of uptake and increasing contrast between prey and coral tissue. Visualization methods using fluorescent polystyrene microbeads first emerged as a biomedical diagnostic tool (Popielarski et al. 2005; Madden et al. 2013; Bott 2014) and have since been applied to investigate prey preference in ornamental marine fish (Lee et al. 2018). Many zooplankton species, including copepods, rotifers and mysid shrimp, graze on particulate matter and inadvertently ingest microplastics. Direct detection of microplastics ingestion in experimentally infected zooplankton has been demonstrated by the application of fluorescent polystyrene microbeads (Setälä et al. 2014; Lee et al. 2018; Miller et al. 2020). These studies suggest that many zooplankton species can be readily incubated with fluorescent microbeads (Setälä et al. 2014; Lee et al. 2018; Miller et al. 2020).

To aid in the direct quantification of feeding rates, this study compares the capture and ingestion abilities of three morphologically distinct scleractinian coral species (*Acropora millepora*, *Pocillopora acuta* and *Galaxea fascicularis*) fed *Artemia* nauplii. Furthermore, this study compares and develops methods that can accurately inform feeding regimes for corals in aquaculture. The ability of these corals to capture and ingest *Artemia* was investigated through two experiments. The first, referred to as “the capture rate experiment,” compared the ability of corals to capture *Artemia salina* instar I nauplii supplied at different initial densities, as measured by the number of prey items cleared from a fixed volume of water. The second experiment, referred to as “the ingestion experiment,” directly quantified the number of prey items ingested by coral polyps via fluorescence microscopy detection of *Artemia* instar II nauplii, incubated with fluorescent microbeads.

## Methods

### Coral collection and maintenance

Three adult colonies (genotypes) of each species (*A. millepora*, *P. acuta* and *G. fascicularis*) were collected from Davies Reef (lat.: 18°49'31" S, long.: 147°38'50" E) (AIMS General Permit G12/35236.1). Following collection, corals were transported to the National Sea Simulator (SeaSim) located at the Australian Institute of Marine Science (AIMS, Cape Cleveland, Australia) and acclimated to aquarium conditions in outdoor tanks for two weeks, with the temperature set to emulate reef conditions (24 °C) at the time of collection.

Adult colonies were cut into small fragments (2–5 cm length) using a Gryphon Coral Saw then adhered to either aragonite (capture rate experiment) or ceramic plugs with a wax coating to prevent biofouling (ingestion experiment). Plugs were placed on elevated PVC trays, which were moved to 250 l indoor holding tanks where fragments further acclimated for four weeks. Holding tanks were supplied with filtered (1 µm) flow-through seawater and a circulation pump (Tunze® Turnbelle® nanostream®) for water movement. The temperature of the holding tanks was maintained at 27 ± 0.02 °C, and a light regime was programmed to match the natural day and night cycle and oscillations in intensity (maximum 200–250 µmol photons m<sup>-2</sup> s<sup>-1</sup>). Lights were ramped up to maximum intensity over four hours, held for four hours then ramped down over four hours. Coral fragments in holding tanks were fed low concentrations of *Artemia* instar I nauplii and *Brachionus plicatilis* daily to support their nutritional health prior to experimental trials. To control algal growth, tanks were manually cleaned weekly as well as via herbivorous snails (*Turbo* spp. and *Thalotia strigata*) and orange-shoulder surgeonfish (*Acanthurus olivaceus*).

### *Artemia* preparation

*Artemia salina* cysts (Sep-Art magnetic GSL *Artemia* cysts, INVE, Belgium) were hatched overnight and harvested daily (2.5 g cysts in 1 l seawater; pH:8, salinity 25–35 ppt). A magnetized collector tube (Sep-Art™, INVE, Belgium) separated cysts from hatched nauplii. Newly harvested instar I nauplii were diluted with filtered seawater (1 µm) and gently aerated (~ 1:4 *Artemia* to seawater ratio; ~ 600 ind. ml<sup>-1</sup>). Repeat counts of *Artemia* nauplii in the diluted solution ( $n=5$  or until the standard error was < 10% of the mean) were conducted in a Bogrov counting chamber to determine the delivered prey densities. The diluted *Artemia* solution was kept at 27 ± 0.02 °C until the feeding trials.

An initial study was conducted to determine an average time point (hours post-harvest) when all *Artemia* had

ingested fluorescent microbeads and their average size at this time. For the ingestion experiment, *Artemia* were harvested at this time point to ensure that they could ingest microbeads and hence could be visualized in fed corals. At eight fixed time points after harvest, *Artemia* nauplii were incubated with fluorescent microbeads, as described below. After incubations, nauplii were placed onto glass cavity slides with the addition of a viscous solution (1% methocel) to slow down prey movement for visualization using an inverted fluorescent microscope (LEICA DMI6000B, LAS-X software) with fluorescent filters (ET-GFP, 450/490 nm) and images were taken (AxioCam MRc Rev. 3). Lengths of nauplii ( $n=30$ ) were measured from the eye to the end of the tail (Ekonomou et al. 2019) using Leica Application Suite X (LAS-X) microscope software. Larval developmental stage was determined by detection of fluorescence beads in the nauplii guts since microbeads could only be taken up by feeding nauplii, which occurs after their first molt into instar II nauplii, with developed mouthparts and guts.

For the ingestion experiment's feeding trials, prior to use, small volumes of the microbeads stock solution ( $3.8 \times 10^{10}$  particles ml<sup>-1</sup>, in a 2% solids solution) were dispensed and diluted with ultra-filtered seawater (0.22 µm) at 1:1 ratio. The diluted solution was sonicated briefly to prevent aggregation, and then, 10 µl was added to 25 ml suspension culture flasks with vented caps (Sarstedt, Germany) with 7 ml of *Artemia* nauplii (~ 600 ind. ml<sup>-1</sup>). Flasks were placed on an orbital shaker (50 rpm) for 1 h before rinsing thoroughly with seawater using a 250 µm mesh net for 5 min. To assess if the washing step removed microbeads from nauplii surfaces and the surrounding solution, aliquots of *Artemia* were fixed in 4% neutral buffered formaldehyde (NBF) in seawater solution before and after and subsequently inspected by fluorescence microscopy. Similarly, an *Artemia* aliquot was fixed after each feeding trial to confirm gut retention of microbeads for downstream detection.

### Feeding trials

Prior to feeding trials, coral fragments were moved into 2.5 l cylindrical acrylic feeding chambers to acclimate for 24 h with flow-through filtered seawater set to one turnover per hour (2.5 l h<sup>-1</sup>). Feeding chambers were placed in freshwater baths to maintain constant temperature of 24 °C. Water powered, magnetic stirrers and a magnetic stir bar were added to the bottom of each feeding chamber to homogenize delivered prey and provide water movement.

Water flow to the feeding chambers was stopped and the water volume in each chamber carefully adjusted by siphoning to 2 l (capture rate experiment) or 1 l (ingestion experiment). Feeds were delivered to the feeding chambers via syringe. Magnetic stir bars (80 revolutions min<sup>-1</sup>) ensured distribution of prey without stratification. Observations on feeding

response indicators (e.g., polyp extension, tentacle movement, formation of mucus-prey agglomerations) were taken at 10 min post-feed delivery as well as throughout each trial.

#### Capture rate experiment

A drop of suspended *Artemia* was added to each chamber to elicit a feeding response prior to delivering feeds. For *P. acuta* and *A. millepora* trials, instar I nauplii were delivered to nine chambers per species, each housing one coral fragment, per prey density treatment (3 replicate chambers per treatment: Low (1 ind. ml<sup>-1</sup>), Medium (2 ind. ml<sup>-1</sup>) and High (4 ind. ml<sup>-1</sup>). For *G. fascicularis* trials, an additional prey density treatment (8 ind. ml<sup>-1</sup>) was added due to the high feeding rates previously documented for *G. fascicularis* (Osinga et al. 2008; 2012b). For each experimental chamber with coral, there was a corresponding control chamber without coral. Trials commenced at 10:00 h, during peak light intensity, on three consecutive mornings. This controlled for potential differences in feeding based on light intensity fluctuations and repeat capture rate measurements over consecutive days tested satiation effects (e.g., decreases in mean daily capture rates over time). Initial ( $C_0$ ) and final ( $C_t$ ) prey concentrations were determined by counting 20 ml seawater aliquots collected five min after feed delivery and again one hour later.

Upon conclusion of the third day of trials, polyp counts were obtained for each fragment. *A. millepora* and *P. acuta* polyp counts were derived by multiplying their respective average number of polyps per square centimeter with their surface area measured using a wax dipping protocol (Veal et al. 2010). The average number of polyps per square centimeter for *A. millepora* and *P. acuta* fragments was estimated by counting the number of polyps within a measured area using ToupView software version 4.10 (ToupTek, Zhejiang, China) from a minimum of three different sections (e.g., base, trunk, branch) of 20 representative fragments per species. Due to their larger size, *G. fascicularis* polyps were counted manually. Mean capture of *Artemia* per coral polyp was calculated by the following Eq. (1):

$$\text{Capture rate} : (C_0 - C_t) \times V_{\text{water}} / N \quad (1)$$

where  $C_0$  is the initial, and  $C_t$  is the final number of nauplii in a sample volume of water at the end of an allocated feeding time (1 h),  $V_{\text{water}}$  is the volume of water in the feeding chamber, and  $N$  is the number of coral polyps (Osinga et al. 2012b).

#### Ingestion experiment

*Artemia* instar II nauplii, incubated with fluorescent microbeads as described above, were delivered at a fixed density (3 ind. ml<sup>-1</sup>) to four replicate feeding chambers per

species. Each chamber housed three fragments of different genotypes ( $n = 12$  fragments per species; four of each genotype). To calculate capture rates for the corals in the same chambers, initial and final prey counts were taken from 20 ml seawater aliquots collected immediately after feed delivery and again 70 min later, allowing 10 min for corals to elicit a feeding response to added prey.

After feeding trials were completed, coral fragments were fixed for 24 h in 4% NBF at 4 °C and then rinsed in ultra-filtered seawater (0.22 μm) prior to placement in 4% formic acid solution for decalcification for 24 h–48 h. Decalcified fragments were rinsed in ultra-filtered seawater (0.22 μm) and placed in 2×PBS in 50% ethanol (0.44 μm syringe filtered) for storage at –20 °C until dissected.

Decalcified corals were pinned to wax dissecting plates using headless stainless-steel pins (5 mm, Cat. no. E185, Australian Entomological Supplies<sup>PTY LTD</sup>) and dissected under a dissecting stereoscope (LEICA MZ109) with an in-built GFP long-pass filter (LEICA ET-GFP LP FLUO filter; excitation filter: 480/40 nm, barrier filter: 254/511 nm) using forceps, dissecting scissors, scalpels, and fine tip dissecting probes (0.25 mm, product 10,140, Fine Science Tools, Inc.). Decalcified corals were cut into tissue sections and imaged one section at a time (Software: LAS V4, Camera: Leica DFC450 C). After imaging, ingested *Artemia* were counted within all the polyps present within each tissue section. Lastly, tissue sections were discarded to avoid double counting.

*Acropora millepora* fragments (L: ~2 cm, W: ~0.5 cm) were incised longitudinally with the axial corallites bisected. *P. acuta* fragments (L: ~2 cm, W: ~2 cm) were ‘unfolded’ and flattened. Each fragment was cut into  $6 \pm 2$  sections. *G. fascicularis* fragments (L: ~2 cm W: ~2 cm) each had four to five polyps, which were dissected separately. The mouth of each *G. fascicularis* polyp was probed to separate clumps of *Artemia* from the tentacles, which auto-fluoresced. Each polyp was then longitudinally incised, flattened and pinned to the wax dish. The flattened sections were further divided to avoid double counting. A series of images were taken for all dissected samples and imported into Image J (<https://imagej.nih.gov/ij/>) for analysis and annotation. In each section, polyps were outlined and numbered with prey enumerated using the multi-point tool. Correct detection of ingested *Artemia* was ensured by comparison with control images generated in pilot studies where corals were delivered (i) *Artemia* without beads; (ii) *Artemia* incubated with beads or (iii) beads only.

#### Data analysis

Statistical analyses were carried out in R-studio (version 1.4.1106, R Core Development Team, 2009) using a significance level of  $P < 0.05$ . Models that best explained

the trends in the feeding rate data, outlined below, were selected using Akaike Information Criterion (AIC). For the capture rate experiment, maximum-likelihood models were used to evaluate the effect of day and initial prey densities (ind. ml<sup>-1</sup>) on capture rates (ind. polyp<sup>-1</sup> h<sup>-1</sup>) (car, lme4 R-packages). Two sets of models were fitted. One examined the effects of coral species, day (i.e., satiation) and initial prey density on the prey capture rate and all interactions. This first model was then reduced to the simplest model, using AIC to compare alternative models. To clarify the significant interactions identified in the final model, each species was then analyzed separately. Additionally, the difference in initial and final *Artemia* nauplii concentrations between control chambers (*Artemia* only) and experimental chambers (*Artemia* + corals) was assessed by paired t tests.

For the ingestion experiment, count regression models assessed the effect of genotype and feeding chamber on the number of *Artemia* counted within polyps of each dissected section of a particular species. Dissected sections within samples were included as random effects, when this was found to improve the model. Overdispersion in the nauplii counts was handled by using the negative binomial as the family for the count regression. Analyses of deviance (car R-package) determined whether the two main effects (genotype, chamber) influenced the number of *Artemia* consumed by each species. Paired t tests assessed differences in feeding rates as calculated by capture rate and ingestion rate values for a given chamber. Lastly, pairwise two-sample t tests, allowing for unequal mean variances, were used to analyze the mean feeding rates from both experiments where initial prey densities were comparable to 3 ind. ml<sup>-1</sup> ± 1.5 to compare results derived from three calculations.

## Results

### *Artemia* developmental stages

For the capture rate experiment, the average length of delivered *Artemia* nauplii was 508 ± 45 µm (instar I, 3 h post-harvest). For the ingestion experiment, *Artemia* were delivered after 22 h post-harvest, as initial trials showed that all nauplii had undergone a first molt into instar II nauplii at this time with an average length of 735 ± 94 µm (Online Resource 1). Observations via fluorescence microscopy found that *Artemia* instar II nauplii ingested fluorescent microbeads and retained their gut contents 2 h post-rinsing, confirming that the fluorescent markers were not lost through excretion during the feeding trials.

### Experiment I: capture rate

For *A. millepora*, the average surface area of fragments was 84 ± 4.5 cm<sup>2</sup>, with an average number of 46 ± 2 polyps cm<sup>-2</sup> (3844 ± 219 mean polyps fragment<sup>-1</sup>) (Table 1). There was no significant difference in initial *Artemia* prey counts between control and experimental chambers ( $t = -0.75$ ,  $df = 52$ ,  $P = 0.5$ ) and no significant difference between initial and final *Artemia* counts in control chambers without corals ( $t = -0.04$ ,  $df = 52$ ,  $P = 0.96$ ). In contrast, a significant difference was found between initial and final *Artemia* counts for chambers with *A. millepora*, with final counts being lower ( $t = 6.39$ ,  $df = 52$ ,  $P < 0.0005$ ). The capture rates of *Artemia* delivered at initial concentrations of 1, 2 and 4 ind. ml<sup>-1</sup> were 0.31 ± 0.08, 0.57 ± 0.08 and 1.22 ± 0.13 ind. polyp<sup>-1</sup> h<sup>-1</sup>, respectively. There was a strong linear relationship between capture rate and prey density as the initial prey concentration increased (capture rate ~ initial ind. polyp<sup>-1</sup>,  $r^2 = 0.88$ ) (Fig. 1a). Capture rates, normalized to polyps across chambers, on consecutive days and delivered prey levels did not differ significantly (Analysis of Deviance,  $\chi^2 = 1.33$ ,  $P = 0.25$  and  $\chi^2 = 3.17$ ,  $P = 0.20$ , respectively). However, coral mucus secretions were observed trapping delivered *Artemia*, particularly in chambers delivered 2 or 4 ind. ml<sup>-1</sup> (Online Resource 2a). There were no significant interactions between fixed factors (Analysis of Deviance,  $\chi^2 = 3.25$ ,  $P = 0.19$ ).

For *P. acuta*, the average surface area of fragments was 153 ± 10 cm<sup>2</sup>, with an average of 70 ± 2 polyps cm<sup>-2</sup> (10,762 ± 748 polyps fragment<sup>-1</sup>) (Table 1). Mean *P. acuta* capture rates ranged from 0 to 0.29 ind. polyp<sup>-1</sup> h<sup>-1</sup> (Fig. 1b). Initial and final *Artemia* counts in the control chambers were not significantly different ( $t = -0.06$ ,  $df = 34$ ,  $P = 0.949$ ) though initial counts made five min after feed delivery were higher in control chambers than in chambers with corals ( $t = 2.73$ ,  $df = 30$ ,  $P < 0.005$ ). In chambers with *P. acuta* fragments, fewer *Artemia* were counted at the final compared to the initial time point ( $t = 3.69$ ,  $df = 22$ ,  $P < 0.005$ ). Mean capture rates when delivered *Artemia* at 1, 2 and 4 ind. ml<sup>-1</sup> were 0.06 ± 0.02, 0.06 ± 0.01 and 0.14 ± 0.09 ind. polyp<sup>-1</sup> h<sup>-1</sup>, respectively. Mean capture rates across chambers on consecutive days and delivered prey levels did not differ significantly (Analysis of Deviance,  $\chi^2 = 1.73$ ,  $P = 0.22$  and  $\chi^2 = 1.33$ ,  $P = 0.30$ , respectively).

*Galaxea fascicularis* fragments had an average of 103 ± 5 polyps (Table 1). Mean *G. fascicularis* capture rates ranged from 1 to 110 ind. polyp<sup>-1</sup> h<sup>-1</sup> in experiments performed on consecutive days (Fig. 1c). The initial and final *Artemia* counts in control chambers as well as initial *Artemia* counts in control and experimental chambers did not differ significantly ( $t = -0.75$ ,  $df = 52$ ,  $P = 0.5$  and  $t = -0.04$ ,  $df = 52$ ,  $P = 0.96$ , respectively). Significantly fewer *Artemia*

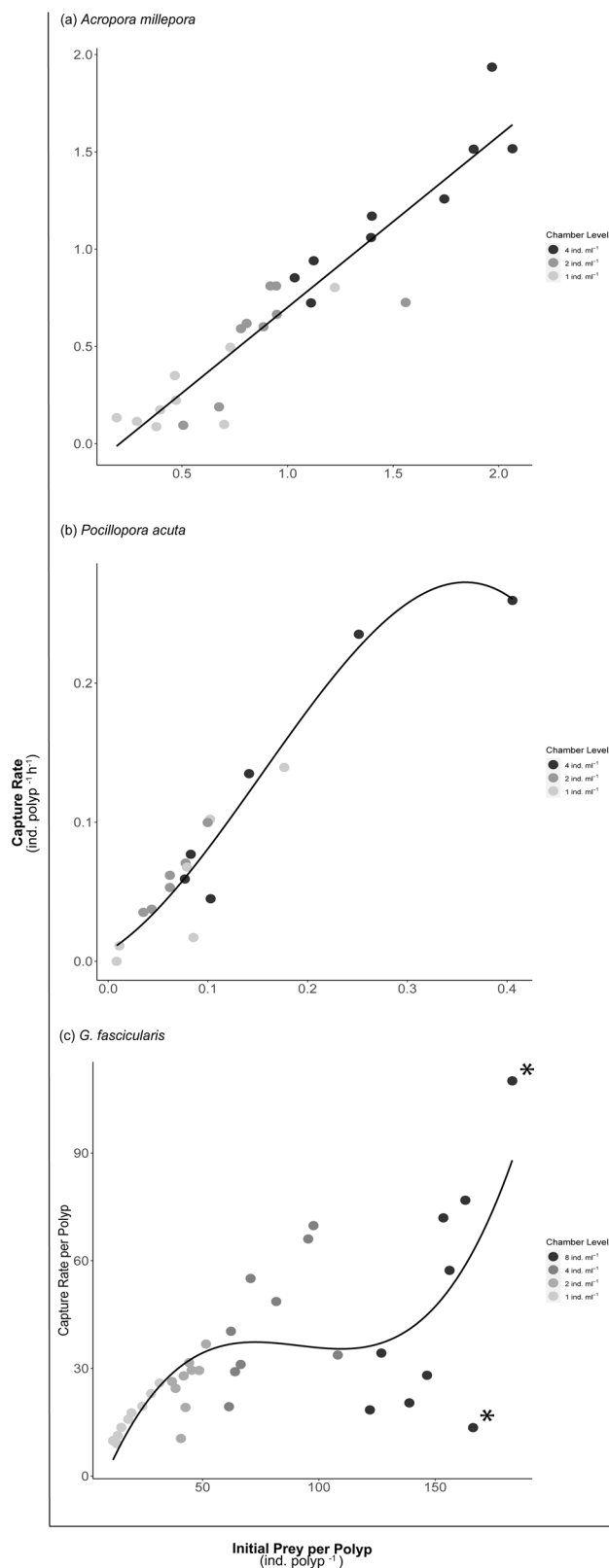
**Fig. 1** Relationship between capture rate and initial prey per polyp in corals fed *Artemia* Instar I nauplii. The x-axis shows number of prey items normalized to polyps per coral fragment ( $\text{ind. polyp}^{-1} \text{h}^{-1}$ ), and the y-axis is the number of prey caught per polyp over an hour from one coral within a chamber on any given day ( $\text{ind. polyp}^{-1}$ ). In *G. fascicularis* trials (c) there was an interaction between day and level on capture rates. The (\*) shows an outlier where the day one capture rate was 110, and day three capture rate was 13.5, from the same coral fragment

were counted for the final compared to the initial time point for chambers containing *G. fascicularis* ( $t=2.95$ ,  $df=67$ ,  $P<0.005$ ). Delivered prey density had a significant effect on capture rates (Analysis of Deviance,  $\chi^2=25.04$ ,  $P<0.001$ ) and were found to be  $16.15 \pm 1.69$ ,  $26.16 \pm 2.20$ ,  $43.67 \pm 5.01$  and  $47.87 \pm 9.56$   $\text{ind. polyp}^{-1} \text{h}^{-1}$  for initial *Artemia* densities of 1, 2, 4 and 8  $\text{ind. ml}^{-1}$ , respectively. Capture rates were not influenced by day (Analysis of Deviance,  $\chi^2=1.58$ ,  $P=0.21$ ), but there was a significant interaction between day and delivered prey level indicating effects of an outlier (Analysis of Deviance,  $\chi^2=20.46$ ,  $P<0.001$ ). Capture rates from a single *G. fascicularis* fragment in one chamber equated to 110 on day one and 13.5 prey captured per polyp on day three.

## Experiment II: ingestion

Dissection of coral polyps fed instar II *Artemia* nauplii with fluorescent microbeads identified variation in prey ingestion between coral species. For *A. millepora*, the total number of polyps assessed over the 12 fragments was 477 with an average of  $40 \pm 2$  polyps per fragment. Eight of 165 polyps (5% of total polyps) from genotype A fragments had ingested *Artemia*, with between 1 and 3 *Artemia* detected per polyp. Two of 150 polyps (1.3% of total polyps) from genotype B fragments were detected to have ingested *Artemia*, with 2 *Artemia* detected per polyp. In contrast, 45 out of 162 polyps from genotype C fragments ingested *Artemia*, with the number of *Artemia* ranging from 1 to 4 per polyp. The fragments from genotype C were observed to have full polyp extension at 10 min post-feed delivery and were noticeably paler than the fragments sourced from other adult colonies. A negative binomial count regression model was found to be the best fit for the *A. millepora* dataset. Genotype significantly influenced the *Artemia* counts in dissected *A. millepora* polyps (Analysis of Deviance,  $\chi^2=15.6$ ,  $P<0.0005$ ), and there was also a significant interaction between genotype and chamber (Analysis of Deviance,  $\chi^2=29.8$ ,  $P<0.0005$ ) (Table 2) (Fig. 2a).

For *P. acuta*, data were collected from 1443 polyps within 72 sections of 12 fragments, with an average of  $3.3 \pm 0.1$  *Artemia* per polyp. A negative binomial mixed-effects model with genotype and chamber as fixed effects was found to be the best fit for the *P. acuta* dataset. Effects of



chamber and genotype did not improve the model, however adding in section as a random effect did (Car package R) (Table 2) (Fig. 2b). This is consistent with the observation

**Table 1** Summary of mean surface area, polyp number and capture rates of corals fed *Artemia* instar I nauplii

Species <sup>a</sup>	Surface area (cm <sup>2</sup> )	No. Polyps		Conc. of nauplii (ind. ml <sup>-1</sup> )	Capture rate <sup>b</sup> (ind. polyp <sup>-1</sup> h <sup>-1</sup> )
		cm <sup>-2</sup>	fragment <sup>-1</sup>		
<i>Acropora millepora</i>	84 ± 4.5	46 ± 2.4	3844 ± 219	1	0.31 ± 0.08
				2	0.57 ± 0.08
				4	1.22 ± 0.13
<i>Pocillopora acuta</i>	153 ± 10	70 ± 2	10,762 ± 748	1	0.06 ± 0.02
				2	0.06 ± 0.01
				4	0.14 ± 0.09
<i>Galaxea fascicularis</i>	n/a	n/a	103 ± 5	1	16.15 ± 1.70
				2	26.16 ± 2.20
				4	43.67 ± 5.01
				8	47.87 ± 9.56

<sup>a</sup>Individual corals were placed in triplicate chambers per prey concentration level (ind. ml<sup>-1</sup>) and fed over three successive days

<sup>b</sup>Capture rates are expressed as Mean ± S.E

that *Artemia* were clumped within polyps and that polyps closer together consumed similar numbers of *Artemia* prey. *Artemia* clusters were typically present in the polyps furthest away from the fragment's point of attachment to the ceramic plug (Online Resource 2b).

For *G. fascicularis*, strong auto-fluorescence in replicate fragments taken from two out of the three adult colonies (i.e., two out of three genotypes) prevented enumeration of ingested prey because *Artemia* was unable to be distinguished from the coral tissue. However, in four replicate fragments taken from a third adult colony (i.e., one genotype), *Artemia* was able to be enumerated without auto-fluorescence interfering. The average prey counts within these replicate fragments were 75 ± 13 ind. polyp<sup>-1</sup> h<sup>-1</sup> ( $n = 20$  polyps).

### Comparison of capture and ingestion rates

Both capture rates and ingestion rates were determined in experiment II to enable direct comparison between these two measures of coral feeding. When normalized to the total number of polyps in the chamber (i.e., across three fragments), the measured capture and ingestion rates differed significantly for *A. millepora* and *P. acuta* but were similar for *G. fascicularis* (Fig. 3). For *A. millepora*, capture rates were higher than ingestion rates ( $t_{\text{one-tail}} = 2.99$ ,  $df = 4$ ,  $P < 0.05$ ), while the opposite was seen for *P. acuta* ( $t_{\text{one-tail}} = -14.84$ ,  $df = 4$ ,  $P < 0.0005$ ). For *G. fascicularis*, capture and ingestion rates were not significantly different ( $t_{\text{one-tail}} = -0.83$ ,  $df = 6$ ,  $P = 0.21$ ). For the latter coral species, the measured rates were based on counts from only one fragment per chamber due to tissue auto-fluorescence in the fragments from the other two genotypes.

### Discussion

Most aquarium-based feeding studies have calculated coral feeding rates from indirect capture rate methods (Petersen et al. 2008; Osinga et al. 2012b; Tagliafico et al. 2018a). However, direct approaches, such as calculating ingestion rates from prey enumerated in polyp dissections, produce more accurate feeding rates and provide insights into how prey is ingested across the entire coral (Sebens et al. 1998; Kuanui et al. 2016). Ingested prey is often difficult to differentiate from coral tissue, and visual markers are one way of mitigating this constraint. Here, visualization of ingested prey was achieved by incubating them with fluorescent microbeads prior to feeding the corals.

### Cross-species and cross-study capture rate comparisons

Results from the capture rate experiment suggest that different coral species have varying abilities to capture delivered *Artemia salina* instar I nauplii. The capture rates increased with prey density level for *A. millepora* and *P. acuta*; however, for these coral species the trend was only significant when capture rates were normalized to polyps per fragment. In contrast, for *G. fascicularis*, the delivered prey density treatment was found to be a significant factor for *Artemia* capture rate, without normalization based on polyp number. The fixed density levels were relatively similar (1–4 ind. ml<sup>-1</sup>), which partly explains why normalization was required for the resulting capture rates to display significant differences. Our results confirm previous studies where capture rates of *Artemia* by corals increased with higher initial prey densities, normalized to polyps per fragment (Petersen et al. 2008; Osinga et al. 2012b; Tagliafico et al. 2018a). Furthermore, given the large number of polyps per *A. millepora*

**Fig. 2** Mean *Artemia* instar II nauplii per (a) *Acropora millepora* ( $n=477$ ) and (b) *Pocillopora acuta* ( $n=1443$ ) polyps in 12 fragments from four feeding chambers and three genotypes (A, B, C). Significant effects of genotype and chambers (“One,” “Two,” “Three,” “Four”) on the response variable, prey nauplii counts were assessed per species

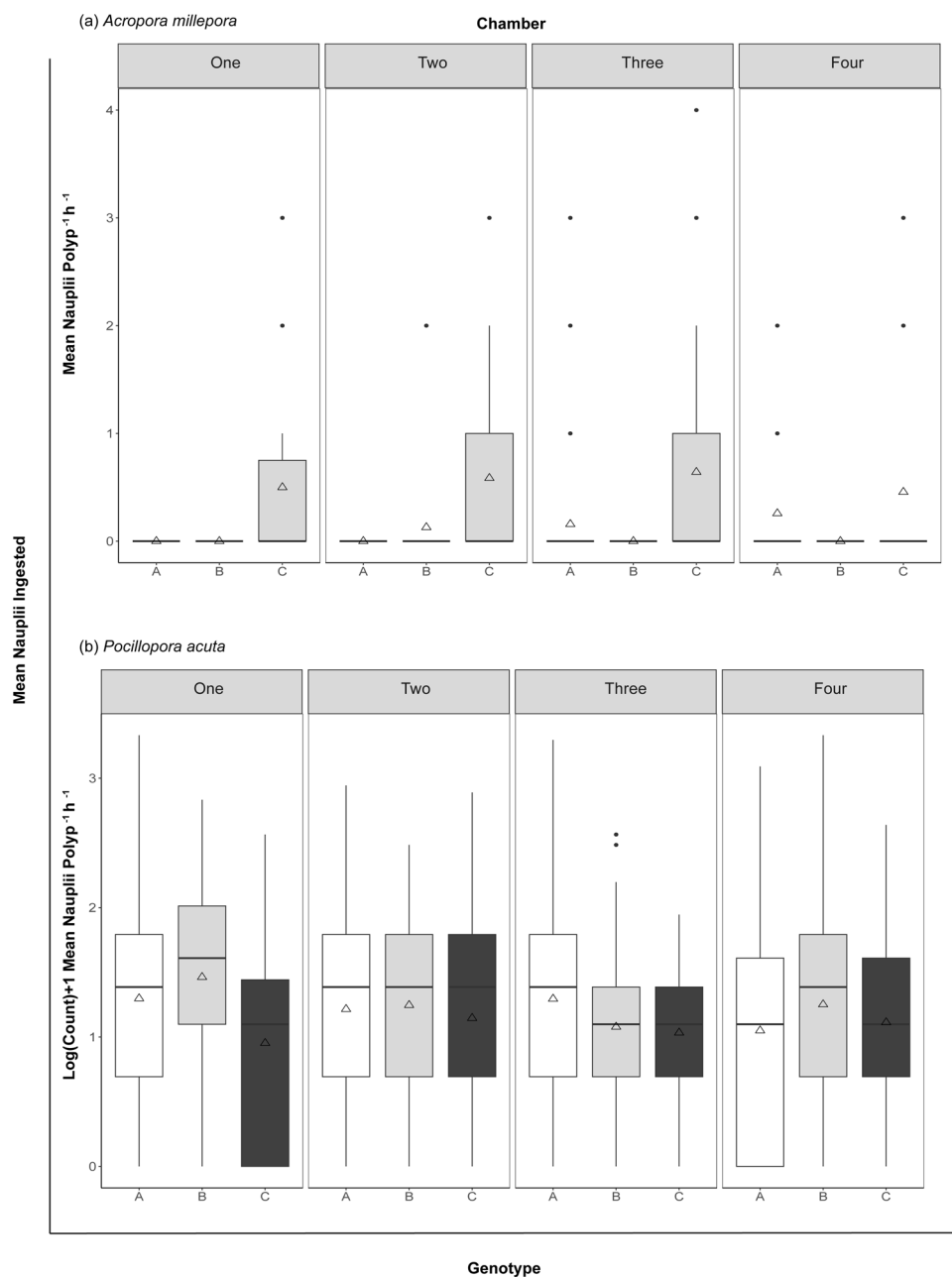


**Table 2** Analysis of Deviance table for the best fit fixed and mixed effect models of the number of *Artemia salina* instar II nauplii ingested by *Acropora millepora* and *Pocillopora acuta*

	×2	df	<i>p</i> value <sup>a</sup>
<i>Acropora millepora</i>			
Genotype	15.6	2	<0.0005 ***
Chamber	2.05	3	0.56
Genotype x chamber	29.8	6	<0.0005***
<i>Pocillopora acuta</i>			
Genotype	4.54	2	0.1
Chamber	2.83	3	0.4
Genotype x chamber	7.29	6	0.3

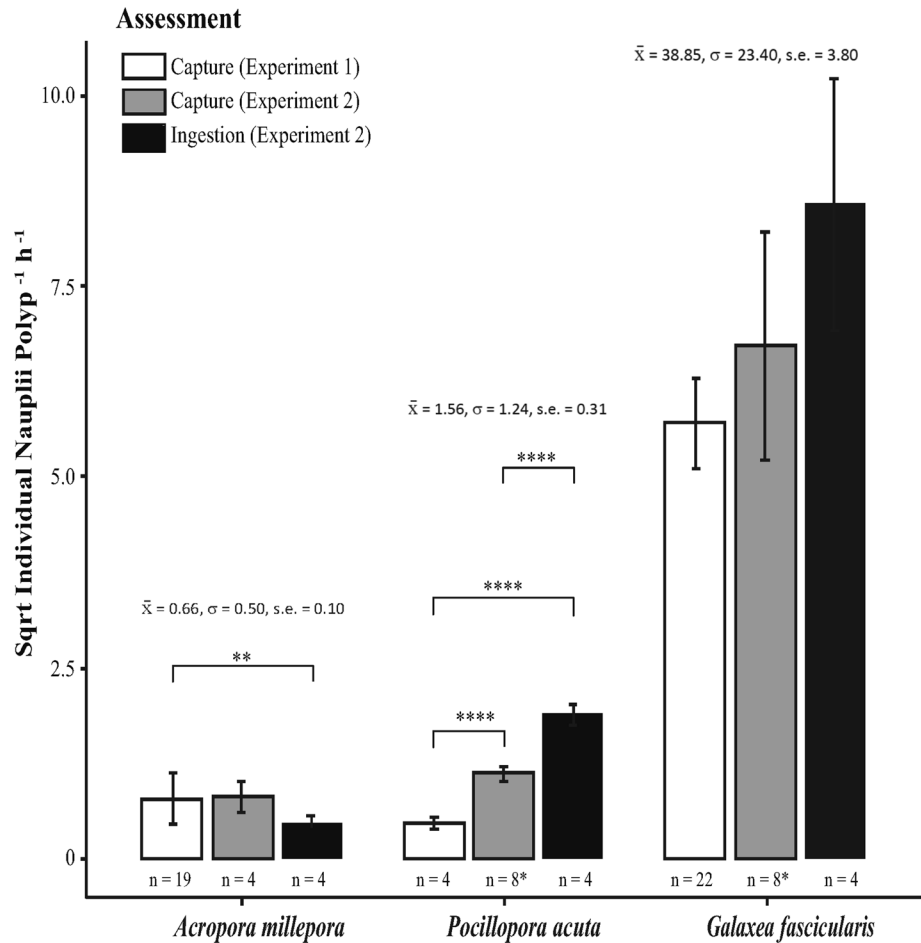
<sup>a</sup>Signif. codes: 0 ‘\*\*\*’ 0.001 ‘\*\*’ 0.01 ‘\*’ 0.05 ‘.’ 0.1 ‘.’ 1

( $x=3844$ ) and *P. acuta* ( $x=10,762$ ) fragments, satiation was not reached at these low-density levels.

*Galaxea fascicularis* has larger polyps and lower surface area to volume ratios than the other coral species in this study. *G. fascicularis* fragments in the capture rate experiment had on average of 103 polyps per fragment, and the delivered prey density was found to be a significant factor of *Artemia* capture rate. *G. fascicularis* is a fast-feeding coral which requires high numbers of *Artemia* for satiation (Osinga et al. 2012b; Tagliafico et al. 2018a), and, except for one fragment that consumed a mean 110 ind. polyp<sup>-1</sup> h<sup>-1</sup> on day one and 13.5 ind. polyp<sup>-1</sup> h<sup>-1</sup> on day three, satiation was not observed here (see Fig. 1c). The differences in *Artemia*



**Fig. 3** Cross-study and cross-species comparison of mean feeding rates in corals derived from feeding chambers. Mean capture rates from chambers with initial instar I nauplii prey counts of  $3 \pm 1.5$  ind.  $\text{ml}^{-1}$  are included from the first experiment (Capture Rate Experiment). Mean capture rates and mean ingestion rates from chambers delivered instar II nauplii and 3 ind.  $\text{ml}^{-1}$  are included from the second experiment's chambers (Ingestion Experiment). Significant values adjusted from pairwise Welch two-sample t tests to account for unequal variance of mean feeding rates per chamber. For *Pocillopora acuta* and *Galaxea fascicularis*, an additional four chambers from experiment 2 pilot studies (\*) were included for this analysis



capture rates across our three experimental species are consistent with other aquarium-based studies. For example, fast-feeding corals, such as *G. fascicularis* and *Duncanopsammia axifuga*, have been observed to consume over one hundred *Artemia* nauplii per polyp compared to autotrophic dominant, smaller polyp corals, such as *A. millepora*, or *H. rigida*, which may consume one nauplii per every ten polyps at the same prey densities (Kuanui et al. 2016; Tagliafico et al. 2018a).

In the capture rate experiment, the lower mean capture rates per delivered prey treatments (1, 2 and 4 ind.  $\text{ml}^{-1}$ ), observed in *P. acuta* trials as compared to *A. millepora* trials, was unexpected. *Pocillopora* spp. have been documented to consume significantly more *Artemia* instar I nauplii than *Acropora* spp. (Latyshev et al. 1991; Toh et al. 2013; Hoogenboom et al. 2015; Conlan et al. 2018; Geertsma et al. 2022). However, true *P. acuta* capture rates in this experiment were likely higher than calculated due to prey capture occurring between the time of delivery, and before initial counts were made five minutes later. This is suggested by significantly fewer *Artemia* counted in initial prey counts from experimental chambers than in control chambers. Additionally, given the significantly

higher mean polyp counts per *P. acuta* fragments than *A. millepora*, calculated capture rates may not be a suitable measure for the comparison. At a delivered *Artemia* density of 1 ind.  $\text{ml}^{-1}$  or less, *A. millepora* and *P. acuta* corals in this study captured 0.31 ind.  $\text{polyp}^{-1} \text{h}^{-1}$  and 0.06 ind.  $\text{polyp}^{-1} \text{h}^{-1}$ , respectively, similar to 0.13 ind.  $\text{polyp}^{-1} \text{h}^{-1}$  and 0.05 ind.  $\text{polyp}^{-1} \text{h}^{-1}$  corals reported by Kuanui et al. (2016). A study by Hoogenboom et al. (2015) reported similar capture rates of *Artemia* nauplii delivered to *Acropora* sp., as reported in this study, though in contrast recorded higher capture rates for *P. acuta* at 188 nauplii  $\text{cm}^{-2} \text{h}^{-1}$  (approx. 18 ind.  $\text{polyp}^{-1} \text{h}^{-1}$  based on average polyp density per  $\text{cm}^2$  calculated here). The difference in the *P. acuta* capture rates reported between studies could be attributable to differences in experimental factors, such as flow rates, recently shown to significantly affect prey capture rates in Caribbean species (Geertsma et al. 2022). However, variable *Artemia* capture rates have previously been documented for *Pocillopora* sp. with capture rates from fragments within the same experiment varying significantly based on the collection location; thus, differences could also be attributed to feeding variability between *Pocillopora* spp. or genotypes. (Kuanui et al. 2016).

Regardless, studies repeatedly show that *Pocillopora* spp. readily feed and derive physiological benefits from *Artemia* as compared to unfed counterparts (Raymundo & Maypa 2004; Toh et al. 2013; Huang et al. 2020).

In general, capture rates estimated using the initial prey density per milliliter of seawater result in inconsistent measures across studies. For example, capture rate calculations of *G. fascicularis* delivered *Artemia* instar I nauplii at 2 ind. ml<sup>-1</sup> produced rates of 9 ind. polyp<sup>-1</sup> h<sup>-1</sup> (Osinga et al. 2008), 26 ind. polyp<sup>-1</sup> h<sup>-1</sup> (this study) and 51 ind. polyp<sup>-1</sup> h<sup>-1</sup> (Ferrier-Pages et al. 2010). Similarly, when prey was delivered at 4 ind. ml<sup>-1</sup>, capture rates recorded in this study were 44 ind. polyp<sup>-1</sup> h<sup>-1</sup> compared to 93 ind. polyp<sup>-1</sup> h<sup>-1</sup> in a study by Wijgerde et al. (2011). However, normalizing the initial prey densities to the individual unit of the polyp results in more consistent capture rates across studies. For example, the capture rate calculated for *G. fascicularis* delivered *Artemia* instar I nauplii at a density of between 40 and 100 ind. polyp<sup>-1</sup>, fell between 10 and 70 ind. polyp<sup>-1</sup> h<sup>-1</sup> in this study, which is consistent with capture rates of 15 and 75 ind. polyp<sup>-1</sup> h<sup>-1</sup> by *G. fascicularis* in a different study, using the same initial density range (Osinga et al. 2012b). Delivered prey density does significantly affect capture rate calculations, though normalizing prey densities to individuals per polyp are likely to produce more comparable results across studies looking at multiple species (Online Resource 3).

### Use of visual tools to assess prey ingestion

Determining the ingestion rate of *Artemia* through gut dissections facilitated by fluorescent markers provides a more accurate assessment of feeding. This study confirmed that different coral species have different feeding rates on the same prey (*A. millepora*, 0.2; *P. acuta* 3.5; *G. fascicularis*, 75 ind. polyp<sup>-1</sup> h<sup>-1</sup> at 3 ind. ml<sup>-1</sup>) and showed species-specific patterns in how prey is ingested across the fragment, such as the non-homogenous distribution of ingested prey between polyps observed in *P. acuta*.

*Pocillopora acuta* fragments had clusters of ingested prey in polyps located in the branch tips, and fewer clusters were found in polyps near the point of adhesion to the coral plug, although the mean number of prey ingested per polyp did not differ across replicate fragments. Previous studies have demonstrated that polyps in different colony branch positions exhibit significantly different nutritional profiles with high-energy nutrients catabolized more readily at the edges of colonies, such as branch tips (Conlan et al. 2018). A similar mechanism could be at play in the *P. acuta* fragments, where the polyps at the tips need to consume more prey to meet the higher nutritional demands of proliferating cells. However, if this were the case, actively growing polyps at the base of the fragment, adjacent to the site of excision

from the adult colony, would similarly need to consume more prey. Alternatively, polyps within the tips may benefit from higher surface area exposed to prey, increasing chances of an encounter. This clumped distribution pattern of prey ingestion cannot be observed by capture rate methods, which assume an even consumption of prey by polyps across a fragment, yet this observation has important implications. For example, it may be important to maximize the number of branch tips that have unrestricted exposure to the water column and maximize the vertical height of each fragment when arranging and attaching *P. acuta* fragments to a substrate in aquaculture.

This study further highlights that factors such as genotype and environmental conditions can influence ingestion rates. Here, this was particularly apparent for *A. millepora*, with two of the three *A. millepora* genotypes not displaying feeding responses such as extended tentacles. In these two genotypes, few dissected polyps (10 out of 315) contained ingested prey. In contrast, 45 out of 162 polyps from the third genotype (genotype 'C' in Fig. 2a) contained ingested prey although the proportion of polyps with and without prey varied between fragments, likely explaining the significant interaction between genotype and chamber on *Artemia* counts. Notably, this third genotype contained fragments that were visually paler, indicating a possible stress response. Additionally, these *A. millepora* fragments were the only ones observed to have fully extended tentacles at 10 min post-delivery. Stressed corals displaying bleaching signs may compensate for lowered autotrophic energetic acquisition through increasing heterotrophic feeding (Hughes & Grottoli 2013). Increased assimilation of heterotrophic carbon has been observed in bleached *Montipora capitata* and *Porites lobata* compared to unbleached controls (Hughes & Grottoli 2013), and a similar mechanism may be at play here. Low feeding rates of *Acropora* spp. on *Artemia* instar I nauplii have been postulated to be due to their higher dependence on autotrophic carbon and small polyp size (Tagliafico et al. 2018a, b). By this reasoning, *A. millepora* corals would be less capable of ingesting larger instar II nauplii. Our results indicate that, although possible for *A. millepora* to consume the larger *Artemia* instar II nauplii, ingestion rates are variable and depend on complex genotype and holobiont health factors, such as the need to compensate for lost nutrition during times of stress.

### Development of feeding assessment methods

Whereas the capture rate approach is a quick and efficient metric, a coral's feeding behavior can influence the efficacy of this assessment method. In this study, capture and ingestion rates were calculated from the same feeding event enabling side-by-side comparison, with the mean values calculated by the two approaches differing

significantly for *A. millepora* and *P. acuta*. For *A. millepora*, secretion of high volumes of mucus, which capture and cause agglomeration of *Artemia* (Huettel et al. 2006; Naumann et al. 2009), could explain why the calculated capture rates were significantly higher than the ingestion rates. In contrast, *P. acuta* capture rates were lower than ingestion calculations, though the reason for this pattern is unclear. It may be associated with uneven distribution of feeding polyps across the colony, resulting in a bias dependent on which polyps were chosen to be dissected. For *G. fascicularis*, there was no significant difference between the capture rate and ingestion rate calculations. This could be related to the low sample size for the ingestion rate calculations resulting from the high auto-fluorescent tissues of two of the three *G. fascicularis* genotypes. Because the auto-fluorescence overlapped with the signal emitted from the microbeads, it obscured differentiation between ingested prey and coral tissue and therefore prevented accurate counts of ingested prey. These observations highlight the need to select markers that maximize contrast with auto-fluorescent pigments present in the coral species and genotypes under study.

Understanding species-specific feeding behavior and the amount of prey corals ingest is critically important for the development of improved feeding regimes in coral aquaculture. We recommend that future coral feeding studies utilize visual markers to assess feeding rates in corals fed live prey items. The potential health benefit derived from enriching live feeds depends on the ability of a coral to capture, ingest, digest and furthermore, assimilate nutrients from the feed. Therefore, this approach is particularly suitable for live feeds that are also suitable for nutritional enrichment. Here, we were able to confirm and compare the capture and ingestion rates of *Artemia salina* nauplii using fluorescent microbeads allowing for the direct detection of prey within individual polyps which allowed standardization across studies and comparison between coral species. Corals possess diverse feeding strategies, physiologies and varying degrees of reliance on autotrophic and heterotrophic nutrient acquisition pathways as seen in here and other studies. Future studies could expand the protocols established herein to assess feeding abilities and prey preferences to cater to the nutritional needs of different corals and develop appropriate nutritional supplementation regimes, required for the expansion of coral aquaculture.

**Acknowledgements** This study was made possible by grants provided by AIMS@JCU, the College of Science and Engineering at James Cook University and in-kind support from the National Sea Simulator at the Australian Institute of Marine Science. Furthermore, we would like to thank the National Sea Simulator personnel, Tom Barker, Loni Koukoumftsis and Andrea Severati and volunteer, Natalia Robledo, for technical assistance and support. Lastly, Rhondda Jones is thanked for her assistance with statistical analyses.

**Funding** Open Access funding enabled and organized by CAUL and its Member Institutions.

## Declarations

**Conflict of interest** On behalf of all authors, the corresponding author states that there is no conflict of interest.

**Open Access** This article is licensed under a Creative Commons Attribution 4.0 International License, which permits use, sharing, adaptation, distribution and reproduction in any medium or format, as long as you give appropriate credit to the original author(s) and the source, provide a link to the Creative Commons licence, and indicate if changes were made. The images or other third party material in this article are included in the article's Creative Commons licence, unless indicated otherwise in a credit line to the material. If material is not included in the article's Creative Commons licence and your intended use is not permitted by statutory regulation or exceeds the permitted use, you will need to obtain permission directly from the copyright holder. To view a copy of this licence, visit <http://creativecommons.org/licenses/by/4.0/>.

## References

- Anthony KRN, Fabricius KE (2000) Shifting roles of heterotrophy and autotrophy in coral energetics under varying turbidity. *J Exp Mar Biol Ecol* 2:221–253
- Barton JL, Willis B, Hutson K (2015) Coral propagation: A review of techniques for ornamental trade and reef restoration. *Rev Aquac* 22:1–19
- Borneman E (2009) Aquarium corals: selection, husbandry, and natural history. TFH Publications, New Jersey, USA
- Bott R (2014) Brock biology of microorganisms. Pearson Education Limited, London
- Brafield AE, Llewellyn MJ (1982) Animal energetics. Springer, New York
- Conlan JA, Bay LK, Severati A, Humphrey C, Francis DS (2018) Comparing the capacity of five different dietary treatments to optimise growth and nutritional composition in two scleractinian corals. *PLoS ONE*. <https://doi.org/10.1371/journal.pone.0207956>
- Conti-Jerpe IE, Thompson PD, Wong CWM, Oliveira NL, Duprey NN, Moynihan MA, Baker DM (2020) Trophic strategy and bleaching resistance in reef-building corals. *Sci Adv*. <https://doi.org/10.1126/sciadv.aaz5443>
- Ekonomou G, Lolas A, Castritsi-Catharios J, Neofitou C, Zouganelis G, Tsiropoulos N, Exadactylos A (2019) Mortality and Effect on growth of *artemia franciscana* exposed to two common organic pollutants. *Water*. <https://doi.org/10.3390/w11081614>
- Ezzat L, Towle E, Irisson JO, Langdon C, Ferrier-Pagès C (2016) The relationship between heterotrophic feeding and inorganic nutrient availability in the scleractinian coral *T. reniformis* under a short-term temperature increase. *Limnol Oceanogr*. <https://doi.org/10.1002/lno.10200>
- Ferrier-Pagès C, Rottier C, Beraud E, Levy O (2010) Experimental assessment of the feeding effort of three scleractinian coral species during a thermal stress: Effect on the rates of photosynthesis. *J Exp Mar Biol Ecol* 390:118–124
- Geertsma RC, Wijgerde T, Latijnhouwers KRW, Chamberland VF (2022) Onset of zooplanktivory and optimal water flow rates for prey capture in newly settled polyps of ten Caribbean coral species. *Coral Reefs* 41:1651–1664
- Goulden EF, Hall MR, Bourne DG, Pereg LL, Høj L (2012) Pathogenicity and infection cycle of *Vibrio owensii* in larviculture of

- the ornate spiny lobster (*Panulirus ornatus*). *Appl Environ Microbiol* 78:2841–2849
- Hall NM, Berry KLE, Rintoul L, Hoogenboom MO (2015) Microplastic ingestion by scleractinian corals. *Mar Biol* 162:725–732
- Hii YS, Soo CL, Liew HC (2009) Feeding of scleractinian coral, *Galaxea fascicularis*, on *Artemia salina* nauplii in captivity. *Aquac Int* 17:363–376
- Hoogenboom M, Rodolfo-Metalpa R, Ferrier-Pagès C (2010) Co-variation between autotrophy and heterotrophy in the Mediterranean coral *Cladocora caespitosa*. *J Exp Biol* 14:2399–2409
- Hoogenboom M, Rottier C, Sikorski S, Ferrier-Pagès C (2015) Among-species variation in the energy budgets of reef-building corals: scaling from coral polyps to communities. *J Exp Biol* 218:3866–3877
- Horn D, Miller M, Anderson S, Steele C (2019) Microplastics are ubiquitous on California beaches and enter the coastal food web through consumption by Pacific mole crabs. *Mar Pollut Bull* 139:231–237
- Houlbrèque F, Tambutté E, Allemand D, Ferrier-Pagès C (2004a) Interactions between zooplankton feeding, photosynthesis and skeletal growth in the scleractinian coral *Stylophora pistillata*. *J Exp Biol* 207:1461–1469
- Houlbrèque F, Tambutté E, Richard C, Ferrier-Pagès C (2004b) Importance of a micro-diet for scleractinian corals. *Mar Ecol Prog Ser* 282:151–160
- Houlbrèque F, Ferrier-Pagès C (2009) Heterotrophy in tropical scleractinian corals. *Biol Rev Camb Philos Soc* 84:1–17
- Huang YL, Mayfield AB, Fan TY (2020) Effects of feeding on the physiological performance of the stony coral *Pocillopora acuta*. *Sci Rep*. <https://doi.org/10.1038/s41598-020-76451-1>
- Huettel M, Wild C, Gonelli S (2006) Mucus trap in coral reefs: Formation and temporal evolution of particle aggregates caused by coral mucus. *Mar Ecol Prog Ser* 307:69–84
- Hughes AD, Grottoli AG (2013) Heterotrophic compensation: a possible mechanism for resilience of coral reefs to global warming or a sign of prolonged stress? *PLoS ONE*. <https://doi.org/10.1371/journal.pone.0081172>
- Hughes AD, Grottoli AG, Pease TK, Matsui Y (2010) Acquisition and assimilation of carbon in non-bleached and bleached corals. *Mar Ecol Prog Ser* 420:91–101
- Kuanui P, Chavanich S, Viyakarn V, Park HS, Omori M (2016) Feeding behaviors of three tropical scleractinian corals in captivity. *Tropical Zoology* 29:1–9
- Kumar GR, Babu DE (2015) Effect of light, temperature and salinity on the growth of *Artemia*. *Int J Eng Sci Invention* 4:7–14
- Latyshev NA, Naumenko NV, Svetashev VI, Latypov YY (1991) Fatty acids of reef building corals. *Mar Ecol Prog Ser* 76:295–301
- Leal MC, Ferrier-Pagès C, Petersen D, Osinga R (2016) Coral aquaculture: applying scientific knowledge to ex situ production. *Rev Aquac* 8:136–153
- Lee IS, Ohs CL, Broach JS, DiMaggio MA, Watson CA (2018) Determining live prey preferences of larval ornamental marine fish utilizing fluorescent microspheres. *Aquaculture* 490:125–135
- Madden CJ, Tupone D, Cano G, Morrison SF (2013)  $\alpha 2$  adrenergic receptor-mediated inhibition of thermogenesis. *J Neurol Sci* 33:2017–2028
- Miller ME, Hamann M, Kroon FJ (2020) Bioaccumulation and biomagnification of microplastics in marine organisms: a review and meta-analysis of current data. *PLoS ONE*. <https://doi.org/10.1371/journal.pone.0240792>
- Naumann M, Richter C, El-Zibdah M, Wild C (2009) Coral mucus as an efficient trap for picoplanktonic cyanobacteria: implications for pelagic–benthic coupling in the reef ecosystem. *Mar Ecol Prog Ser* 385:65–76
- Osinga R, Schutter M, Griffioen B, Wijffels RH, Verreth JAJ, Shafir S, Henard S, Taruffi M, Gili C, Lavorano S (2011) The biology and economics of coral growth. *Mar Biotechnol* 13:658–671
- Osinga R, Schutter M, Wijgerde T, Rinkevich B, Shafir S, Shpigel M, Marco Luna G, Danovaro R, Bongiorno L, Deutsch A, Kücken M, Hiddinga B, Janse M, McLeod A, Gili C, Lavorano S, Henard S, Barthelemy D, Westhoff G, Laterveer M (2012a) The CORAL-ZOO project: A synopsis of four years of public aquarium science. *Mar Biol Assoc UK* 92:753–768
- Osinga R, Van Delft S, Lewaru M, Janse M, Verreth J (2012b) Determination of prey capture rates in the stony coral *Galaxea fascicularis*: a critical reconsideration of the clearance rate concept. *Mar Biol Assoc UK* 92:713–719
- Osinga R, Charko F, Cruzeiro C, Janse M, Grymonpre D, Sorgeloos, P (2008) Feeding corals in captivity: uptake of four *Artemia* - based feeds by *Galaxea fascicularis*. In: *Proceeding 11th international coral reef symposium* 1: 149–153
- Palardy JE, Rodrigues LJ, Grottoli AG (2008) The importance of zooplankton to the daily metabolic carbon requirements of healthy and bleached corals at two depths. *J Exp Mar Biol Ecol* 367(2):180–188. <https://doi.org/10.1016/j.jembe.2008.09.015>
- Petersen D, Wietheger A, Laterveer M (2008) Influence of different food sources on the initial development of sexual recruits of reefbuilding corals in aquaculture (vol 277, pg 174, 2008). *Aquaculture* 277:174–178
- Popielarski SR, Pun SH, Davis ME (2005) A nanoparticle-based model delivery system to guide the rational design of gene delivery to the liver. 1. Synth Charact *Bioconjug Chem* 16:1063–1070
- Raymundo LJ, Maypa AP (2004) Getting bigger faster: Mediation of size-specific mortality via fusion in juvenile coral transplants. *Ecol Appl* 14:281–295
- Sebens KP, Grace SP, Helmuth B, Maney EJ, Miles JS (1998) Water flow and prey capture by three scleractinian corals, *Madracis mirabilis*, *Montastrea cavernosa* and *Porites porites* in a field enclosure. *Mar Biol* 131:347–360
- Setälä O, Fleming-Lehtinen V, Lehtiniemi M (2014) Ingestion and transfer of microplastics in the planktonic food web. *Environ Pollut* 185:77–83
- Sheridan C, Kramarsky-Winter E, Sweet M, Kushmaro A, Leal MC (2013) Diseases in coral aquaculture: causes, implications and preventions. *Aquaculture* 396:124–135
- Smith JN, Strahl J, Noonan SHC, Schmidt GM, Richter C, Fabricius KE (2016) Reduced heterotrophy in the stony coral *Galaxea fascicularis* after life-long exposure to elevated carbon dioxide. *Sci Rep*. <https://doi.org/10.1038/srep27019>
- Tagliafico A, Rangel S, Kelaher B, Christidis L (2018a) Optimizing heterotrophic feeding rates of three commercially important scleractinian corals. *Aquaculture* 483:96–101
- Tagliafico A, Rangel S, Kelaher B, Scheffers S, Christidis L (2018b) A new technique to increase polyp production in stony coral aquaculture using waste fragments without polyps. *Aquaculture* 484:303–308
- Toh TC, Peh JWK, Chou LM (2013) Heterotrophy in recruits of the scleractinian coral *Pocillopora damicornis*. *Mar Freshw Behav Physiol* 46:313–320
- Trager G, Achituv Y, Genin A (1994) Effects of prey escape ability, flow speed, and predator feeding mode on zooplankton capture by barnacles. *Mar Biol* 120:251–259
- Veal CJ, Carmi M, Fine M, Hoegh-Guldberg O (2010) Increasing the accuracy of surface area estimation using single wax dipping of coral fragments. *Coral Reefs* 29:893–897
- Wijgerde T, Diantari R, Lewaru MW, Verreth JAJ, Osinga R (2011) Extracoelenteric zooplankton feeding is a key mechanism of

nutrient acquisition for the scleractinian coral *Galaxea fascicularis*. *J Exp Biol* 214:3351–3357

Xu J, Jia H, Cui G, Tong H, Wei J, Shao D, Liu K, Qiu Y, Li B, Ma Z (2018) ICEAplChn1, a novel SXT/R391 integrative conjugative element (ICE), carrying multiple antibiotic resistance genes in *Actinobacillus pleuropneumoniae*. *Vet Microbiol* 220:18–23

**Publisher's Note** Springer Nature remains neutral with regard to jurisdictional claims in published maps and institutional affiliations.